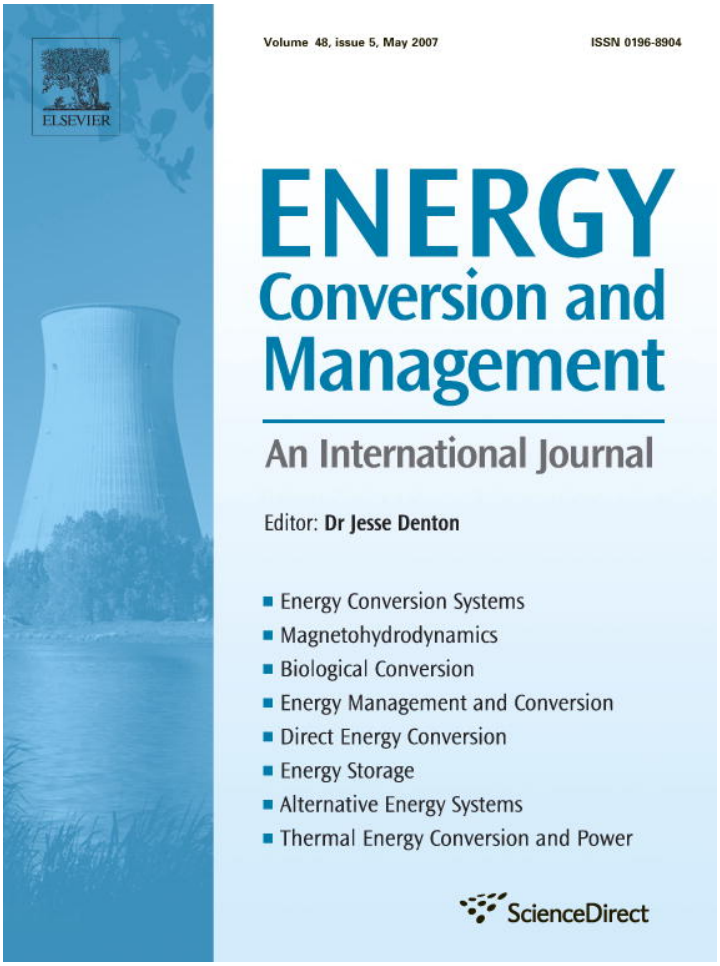

Available online at www.sciencedirect.com
ScienceDirect
Energy Conversion and Management 48 (2007) 1569–1578
ENERGY CONVERSION & MANAGEMENT
www.elsevier.com/locate/enconman

Thermal performance of a micro-combustor for micro-gas turbine system

H.L. Cao [a,b], J.L. Xu [a,*]

[a] Guangzhou Institute of Energy Conversion, Chinese Academy of Sciences, Nengyuan Road, Wushan 510640, PR China
[b] Department of Thermal Science and Energy Engineering, University of Science and Technology of China, Hefei 230026, PR China

Received 8 November 2005; received in revised form 11 May 2006; accepted 26 November 2006
Available online 22 January 2007

Abstract

Premixed combustion of hydrogen gas and air was performed in a stainless steel based micro-annular combustor for a micro-gas turbine system. Micro-scale combustion has proved to be stable in the micro-combustor with a gap of 2 mm. The operating range of the micro-combustor was measured, and the maximum excess air ratio is up to 4.5. The distribution of the outer wall temperature and the temperature of exhaust gas of the micro-combustor with excess air ratio were obtained, and the wall temperature of the micro-combustor reaches its maximum value at the excess air ratio of 0.9 instead of 1 (stoichiometric ratio). The heat loss of the micro-combustor to the environment was calculated and even exceeds 70% of the total thermal power computed from the consumed hydrogen mass flow rate. Moreover, radiant heat transfer covers a large fraction of the total heat loss. Measures used to reduce the heat loss were proposed to improve the thermal performance of the micro-combustor. The optimal operating status of the micro-combustor and micro-gas turbine is analyzed and proposed by analyzing the relationship of the temperature of the exhaust gas of the micro-combustor with thermal power and excess air ratio. The investigation of the thermal performance of the micro-combustor is helpful to design an improved micro-combustor.

Keywords: Micro-combustion; Micro-combustor; Thermal performance; Operating range; Heat loss

1. Introduction

There is an increasing interest in micro-power generation systems for many micro- and mini-devices such as micro-aerial vehicles, micro-robots, portable electronics and micro- and nano-satellites etc. All these systems require a miniaturized power supply with some merits such as high power density, sustaining power supply and small volume and weight. Therefore, the development of micro-power sources or power MEMS (micro-electro-mechanical systems) is quite attractive. A power MEMS, first suggested by Epstein in 1996 [1], is actually a micro-gas turbine generator with less than 1 cm^3 volume by MEMS technology and is desired to produce 10–50 W electrical power while consuming under 10 g/h of hydrogen, whose power density is 10 times higher than that of the best available batteries [2].

The micro-combustor is a key component of the micro-gas turbine generator, where the chemical energy of the fuel is converted to thermal energy of its exhaust gas, which can finally be converted to the output electrical energy. To develop a silicon based micro-gas turbine engine, a six wafer combustor [2,3] with a volume of $\phi 18.4 \times \phi 9.6 \times 1$ mm^3 was developed by Waitz using MEMS technology, and its premixed combustion performance of hydrogen gas was tested. In order to develop a micro-thermo-photo-voltaic power system [4,5], micro-combustion in the stainless steel based micro-tube was performed using a backward facing step to stabilize the flame. Shan [6,7] developed a seven layer silicon wafer micro-combustor and investigated its combustion performance by numerical

* Corresponding author. Tel./fax: +86 20 87057656.
E-mail address: xujl@ms.giec.ac.cn (J.L. Xu).

0196-8904/$ - see front matter © 2006 Elsevier Ltd. All rights reserved.
doi:10.1016/j.enconman.2006.11.022

Nomenclature

C	coefficient
Cp_A	specific heat of air [J (g K)$^{-1}$]
Cp_H	specific heat of hydrogen gas [J (g K)$^{-1}$]
d	diameter of inlet tube of micro-combustor (m)
dA	area of micro-annulus (m^2)
dQ_r	radiant heat loss of micro-annulus (W)
Gr	Grashof number
h	heat transfer coefficient [W (m^2 K)$^{-1}$]
l	characteristic length (m)
M_A	mean molecular weight of air, 28.96
M_H	mean molecular weight of hydrogen gas, 2.0
M_M	mean molecular weight of premixed gas
m_A	mass flow rate of air (g s^{-1})
m_H	mass flow rate of hydrogen gas (g s^{-1})
m_M	mass flow rate of premixed gas (g s^{-1})
n	exponent
P	pressure of fluid through flow meter (Pa)
P_0	calibrated pressure of flow meter (101,325 Pa)
P_A	pressure of air through flow meter (Pa)
P_H	pressure of hydrogen gas through flow meter (Pa)
P_M	pressure of premixed gas (Pa)
Pr	Prandtl number
Q_{nc}	natural convection heat loss (W)
Q_r	radiant heat loss (W)
Q_t	total thermal power (W)
R	gas constant, 8.314 [J (mol K)$^{-1}$]
T	temperature of fluid through flow meter (K)
T_0	calibrated temperature of flow meter (293 K)
T_A	temperature of air through flow meter (K)
T_H	temperature of hydrogen gas through flow meter (K)
T_M	temperature of premixed gas (K)
T_{en}	temperature of environment gas (K)
T_w	measured wall temperature (K)
V	actual volumetric flow rate (m^3 s^{-1})
V'	reading volumetric flow rate (m^3 s^{-1})
V_A	actual volumetric flow rate of air (m^3 s^{-1})
V_H	actual volumetric flow rate of hydrogen gas (m^3 s^{-1})
V_M	actual volumetric flow rate of premixed gas (m^3 s^{-1})

Greek symbols

α	excess air ratio
ε	calibrated emissivity of wall surface of micro-combustor
φ	Stefen–Boltzmann constant, 5.67×10^{-8} [W (m^2 K^4)$^{-1}$]
λ	thermal conductivity [W (m K)$^{-1}$]
η_{nc}	rate of natural convection heat loss
η_r	rate of radiant heat loss
η_t	rate of total heat loss
ΔH_A	enthalpy difference of air
ΔH_H	enthalpy difference of hydrogen gas
ΔS	increasing entropy of premixed gas

simulation and experimental study. Peris [8] developed a stainless steel based micro-axial turbine and investigated its turbine performance. However, to the author's knowledge, the detailed thermal performance of the stainless steel based micro-combustor has not been reported previously. Moreover, as an important parameter used to calculate the heat efficiency of the micro-combustor, the rate of heat loss has only been analyzed qualitatively in some literatures and considered to be much larger than that of the conventional combustor due to the increased ratio of surface area to volume [2]. However, it has not been analyzed and calculated quantitatively.

We are developing a stainless steel based micro-gas turbine generator, and the design of a high performance micro-combustor is the first step. The pressure and temperature of the exhaust gas from the micro-combustor will directly influence the efficiency of the micro-gas turbine. Therefore, obtaining higher temperature of the exhaust gas and combustion efficiency is the goal of designing the micro-combustor. It is important to know whether micro-scale combustion can be maintained in the micro-combustor and to investigate the operating range of the micro-combustor and its thermal performance, including wall temperature and heat loss. Therefore, our present work is to develop a stainless steel based micro-annular combustor and investigate its operating range and thermal performance. The results are helpful to design an improved micro-combustor.

2. Experimental setup and apparatus

Hydrogen was chosen as the optimal fuel for micro-combustion because of its high heating value, short reaction time, rapid rate of vaporization, fast diffusion velocity and high flame speed [9]. As is shown in Fig. 1, the experimental setup consists of two gas pipelines. One is the hydrogen gas pipeline to provide fuel for the micro-combustor, while the other is the air pipeline to provide fresh air. Hydrogen gas, released from the hydrogen can (2), flows through the high precision reducing valve (3) and high precision flow meter (4) and finally enters the premixed chamber (5). Air, from the air stabilizer, flows through the high precision reducing valve (3) and high precision flow meter (4) and finally enters the premixed chamber (5) and mixes fully with the hydrogen gas. The premixed chamber consists of two pipes with different diameters, and there are four 0.5 mm diameter pores located in the inner tube wall. Air flows through

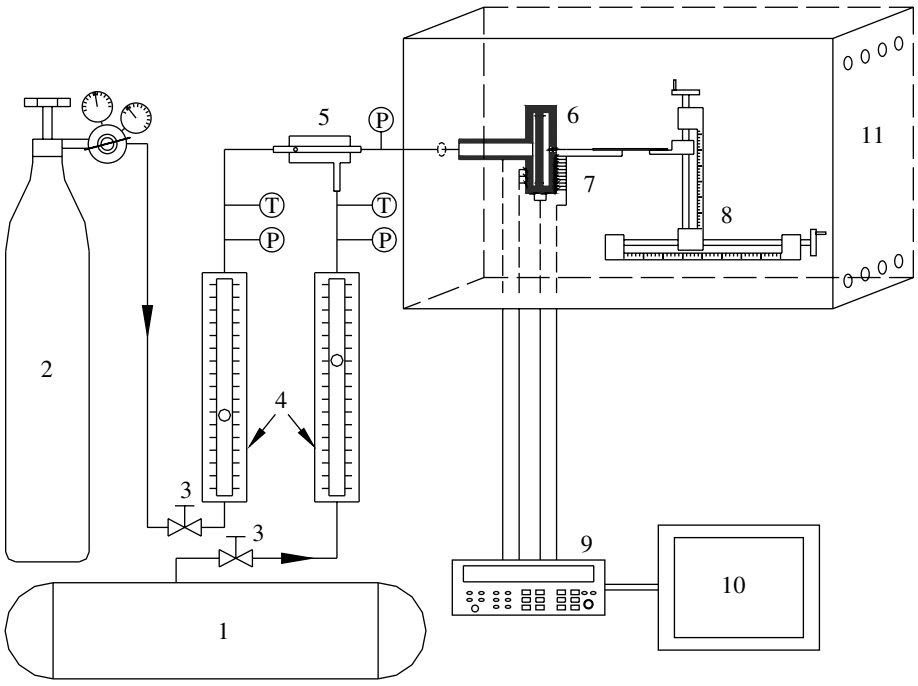

Fig. 1. Experimental setup and apparatus of micro-scale combustion: (1) air stabilizer, (2) hydrogen can, (3) high precision reducing valve, (4) high precision flow meter, (5) premixed chamber, (6) micro-combustor, (7) thermocouple, (8) 2D coordinate measuring instrument, (9) data acquisition, (10) computer, (11) a large glass box.

the annular space between the two pipes, through the micro-pores and jets at high velocity into the inner tube and finally mixes fully with air in the inner tube. Then, the premixed gas enters the micro-combustor and is ignited. The volumetric flow rate of hydrogen gas is measured with the high precision glass flow meter (Cole-Parmer 03227-12) with a capacity of 1021 ml min^{-1}. Two types of glass flow meters, with capacities of 3807 and 8678 ml min^{-1}, are chosen to measure the possibly large range of air volumetric flow rate. The flow rate accuracy of the three types of glass flow meters is within 2% of the full scale. The pressures of the hydrogen gas, air and premixed gas are measured with two kinds of U type tube differential pressure meters with the capacity of 0–1000 mm, while the gas temperatures of the hydrogen gas and air are determined with fine K type jacket thermocouples with the accuracy of ±0.5 K.

A micro-combustor with 26 mm diameter, 9 mm height and 2 mm wall thickness was designed (shown in Fig. 2a). The integral chamber is divided by a 2 mm thick middle disk (II) into two chambers, named inlet chamber (I) and micro-combustion chamber (III). The gaps of the inlet chamber and micro-combustion chamber are 1 mm and 2 mm, respectively, and their diameters are both 22 mm. There are 60 orifices with the diameter of 300 μm evenly distributed at 20 mm diameter circumference in the middle disk. A heating wire with the diameter of 350 μm, located at 18 mm diameter circumference in the micro-combustion chamber is used as the igniter. The premixed gas, out of the premixed chamber, is dispersed in the inlet chamber, then

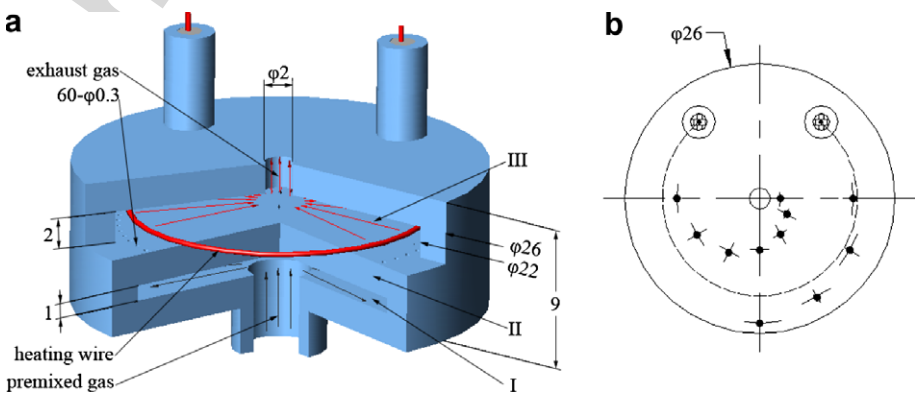

Fig. 2. (a) The 3D configuration of the micro-annual combustor. (I) Inlet chamber, (II) middle disk, (III) micro-combustion chamber. (b) The distribution of the thermocouple on the micro-combustion chamber wall.

Table 1
Calibration of surface emissivity of micro-combustor

T_{tc} (K)	454.8	545.5	652.8	710.2	770.3	824.4	878.9	904.3
T_{IR} (K)	454.7	545.9	653.2	711.3	770.6	825.6	879.6	903.2
ε	0.53	0.54	0.57	0.59	0.63	0.69	0.72	0.72
	$\varepsilon = -0.0879318 + 0.00333731 \times T - 6.13661 \times 10^{-6} \times T^2 + 3.91912 \times 10^{-9} \times T^3$ (453.1 K < T < 873.1 K)						0.72	

jets from the micro-inlet orifices into the micro-combustion chamber and is finally ignited by the igniter. The exhaust gas is discharged from a 2 mm diameter orifice located at the center of the outer combustor wall. The material used for fabrication of the micro-combustor is high quality stainless steel (0Cr17Ni12Mo2).

During the course of experiments, micro-combustor (6) and 2D coordinate measuring instrument (8) are put into a large glass box (11) (Fig. 1) with far larger volume than that of the micro-combustor. By this means, it is assured that the natural convection heat loss of the micro-combustor is not disturbed by the flow of external air.

In order to obtain the temperature fields of the whole micro-combustor, some K type jacket thermocouples with the accuracy of ±0.5 K are fixed on the outer wall of the micro-combustor by point welding. Fig. 2b shows the distribution of thermocouples on the surface of the micro-combustion chamber. The thermocouples are radially distributed with the radius varied from 2 mm, 3 mm, ... to 12 mm. A pair of thermocouples, fixed on a 2D coordinate measuring instrument (8), is used to measure the temperature of the exhaust gas. All the temperatures are collected by the HP high speed data acquisition system (9) and stored in the PC memory (10) for further analysis.

The surface emissivity of the micro-combustor wall is an important factor used to calculate the radiation heat loss and, therefore, must be obtained. In order to determine the surface emissivity of the micro-combustor wall, a calibration of the surface emissivity was performed. The wall temperature of the micro-combustor was measured with K type thermocouples as well as an IR image system (FLIR ThermaCAM SC3000). The surface emissivity could be determined finally by recalculating and resetting until the mean temperature obtained with the IR image system is almost equal to that obtained with the K type thermocouples. By this means, the surface emissivity ε of the micro-combustor wall was determined at different temperatures. As is shown in Table 1, the surface emissivity ε of the micro-combustor wall can be calculated with the cubic polynomial expression when the wall temperature is less than 870 K, and when the wall temperature is greater than 870 K, the surface emissivity is almost equal to 0.72.

3. Data processing and error analysis

The actual volumetric flow rate V of the fluid through the flow meter is calculated in terms of its reading volumetric flow rate V' by

$$V = V' \cdot \sqrt{\frac{P_0 \cdot T}{P \cdot T_0}}, \tag{1}$$

where P_0, T_0 is the pressure and temperature at which the flow meter is calibrated and P, T is the actual pressure and temperature of the fluid through the flow meter respectively. Therefore, adopting the expression, the actual volumetric flow rates V_A, V_H of air and hydrogen gas through the flow meters are calculated in terms of their reading volumetric flow rate V'_A, V'_H, pressure P_A, P_H and temperature T_A, T_H. The two mass flow rates m_A, m_H and their total mass flow rate m_M are easily computed by the ideal gas state equation. The excess air ratio α is defined as the ratio of the actual air mass flow rate to the necessary air mass flow rate for full reaction of the fuel. In fact, it is the reciprocal value of the equivalence ratio. For the reaction of hydrogen gas and air, it is computed as

$$\alpha = \frac{m_A}{m_H \cdot 34.48} \tag{2}$$

where 34.48 is the mass ratio of air to hydrogen gas at the excess air ratio of 1. The molecular weight of the premixed gas is calculated by

$$M_M = \frac{m_H \cdot M_H + m_A \cdot M_A}{m_H + m_A} \tag{3}$$

where M_H, M_A is the molecular weight of hydrogen gas and air, respectively. The specific heat of hydrogen gas and air Cp_H, Cp_A is computed by an interpolation method in terms of each temperature.

From the viewpoint of thermodynamics, the mixing process of hydrogen gas and air in the premixed chamber can be considered as adiabatic, and hence, the laws of energy conservation and mass conservation must be applied for the mixing process of hydrogen gas and air. Therefore, the enthalpy difference of the hydrogen gas ΔH_H must be equal to that of air ΔH_A, that is

$$\Delta H_H = \Delta H_A \tag{4}$$

In the mixing process of hydrogen gas and air, their enthalpy differences ΔH_H, ΔH_A are, respectively, written as

$$\left.\begin{aligned} \Delta H_H &= m_H \cdot Cp_H \cdot (T_H - T_M) \\ \Delta H_A &= m_A \cdot Cp_A \cdot (T_M - T_A) \end{aligned}\right\} \tag{5}$$

Substituting Eq. (5) into Eq. (4), we can obtain Eq. (6)

$$T_M = T_A + \frac{m_H \cdot Cp_H}{m_H \cdot Cp_H + m_A \cdot Cp_A} \cdot (T_H - T_A) \tag{6}$$

and finally, the temperature T_M of the premixed gas is computed in terms of Eq. (6). Hence, the volumetric flow rate of the premixed gas can be calculated by Eq. (7)

$$V_M = \frac{m_M \cdot R \cdot T_M}{M_M \cdot P_M} \quad (7)$$

where R is the universal gas constant and is equal to 8.314 J (mol K)$^{-1}$ and P_M is the measured pressure of the premixed gas. Therefore, the inlet flow rate of premixed gas in the inlet tube of the micro-combustor is finally computed by Eq. (8)

$$u = \frac{4 \cdot V_M}{\pi \cdot d^2} \quad (8)$$

where d is the diameter of the inlet tube of the micro-combustor and is equal to 4.0 mm.

The premixing process of hydrogen gas and air is actually irreversible, and hence, the total entropy of the hydrogen gas and air must increase. The increasing of entropy ΔS of the premixing process is written as

$$\Delta S = Cp_H \cdot \ln\frac{T_M}{T_H} - R \cdot \ln\frac{P_M}{P_H} + Cp_A \cdot \ln\frac{T_M}{T_A} - R \cdot \ln\frac{P_M}{P_A}. \quad (9)$$

In all experiments, because the temperature T_H of the hydrogen gas is almost equal to that T_A of air, the temperature T_M of the premixed gas is also approximately equal to that T_A of air in terms of Eq. (6). Therefore, the increasing of entropy arising from temperature change is almost equal to zero. On the other hand, because the diameter of the tube through which the premixed gas flows is equal to that of the tube through which the hydrogen gas flows, the measured pressure P_M of the premixed gas is almost equal to the pressure P_H of the hydrogen gas. Although the measured pressure P_A of air is a little larger than the P_H of the hydrogen gas, the maximum difference between them is very small in all the experiments. Even under the condition of the highest thermal power and maximum air flow rate, the maximum difference between them is still less than 3000 Pa and 3% of the standard atmosphere pressure. Therefore, the increasing of entropy owing to pressure change is also very small. Thus, the increasing of entropies ΔS of the premixing processes in all experiments is all very small and can even be ignored.

The heat loss of the micro-combustor, consisting of natural convection heat loss and radiant heat loss, can be calculated in terms of the measured wall temperatures of the micro-combustor. Because of the non-uniform temperature of the micro-combustor walls, the natural convection heat loss of the wall is calculated in terms of the average temperature of each wall. In terms of the empirical formula [10], the natural convection heat transfer coefficient h of the micro-combustor wall is written as

$$h = \frac{\lambda}{l} \cdot C \cdot (Gr \cdot Pr)^n \quad (10)$$

where λ, Pr is the thermal conductivity and Prandtl number of air, l is the characteristic length of the wall, Gr is the Grashof number corresponding to the wall temperature. Since the characteristic length of the micro-combustor is in the millimeter magnitude and all the calculated Grashof numbers Gr are less than 5.76×10^8, the outer natural convection of the micro-combustor is regarded as laminar flow, and n is identically equal to 0.25. Because the outer walls of the combustion chamber and inlet chamber are treated as vertical plane plates, C is recommended to be taken equal to 0.59. In addition, the outer annular wall of the micro-combustor is horizontal, hence, C is recommended to be 0.48.

Table 2
Measurement errors

Parameters	Maximum errors	Parameters	Maximum errors
V'_A	2%	m_H	2.02%
V'_H	2%	m_M	2.02%
P_A	10 Pa (0.01%)	α	2.86%
P_H	10 Pa (0.01%)	dA	0.14%
P_M	10 Pa (0.01%)	T_M	0.16%
T_A	0.5 K (0.16%)	Gr	0.24%
T_H	0.5 K (0.16%)	h	0.26%
T_w	0.5 K (0.16%)	dQ_r	0.35%
T_{en}	0.5 K (0.16%)	Q_t	2.02%
l	0.02 mm (0.1%)	η_r	2.05%
V_A	2.01%	η_{nc}	2.05%
V_H	2.01%	η_t	2.88%
m_A	2.02%		

The radiant heat loss is directly proportional to the fourth power of wall temperature and, hence, is greatly sensitive to the change of wall temperature. In order to calculate accurately the radiant heat loss of the micro-combustor, the total radiant heat loss can be calculated with the integrals of the many radiant heat losses of the micro-annulus. In terms of the Stefen–Boltzmann law [10] of radiant heat transfer, the radiant heat loss dQ_r of the micro-annulus corresponding to the micro-annulus's area dA can be calculated as

$$dQ_r = dA \cdot \varepsilon \cdot \varphi \cdot [T_w^4 - T_{en}^4] \quad (11)$$

where ε is the calibrated emissivity of the wall surface of the micro-combustor, φ is the Stefen–Boltzmann constant and is equal to 5.67×10^{-8} W (m^2 K^4)$^{-1}$ and T_w, T_{en} are the measured temperatures of the wall and environment, respectively.

The errors come from the measurement errors of the set of parameters that are listed in Table 2. Performing the standard error analysis, the maximum uncertainties of all the calculated parameters are given in Table 2. It is seen that the maximum errors due to the instrumentation are less than 2.86%, 2.02%, 2.88% for α, Q_t and η_t, respectively.

4. Experimental results and discussion

4.1. Operating range of the micro-combustor

When the electric power of the igniter is increased to a certain value, it is seen that the temperatures of the micro-combustor wall and exhaust gas begin to rise suddenly, and after turning off the power source, the temperatures of the combustor wall and exhaust gas still continue

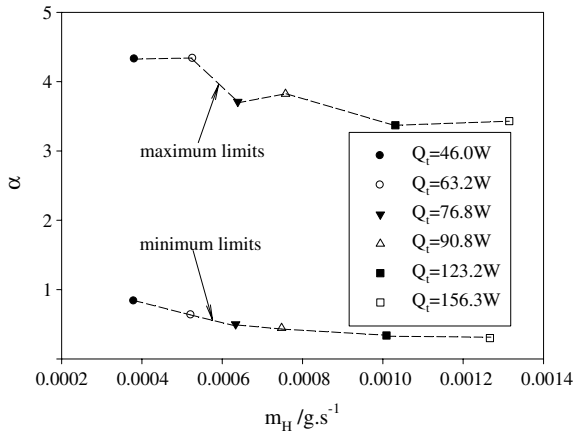

Fig. 3. Operating range of micro-combustor at different thermal powers.

to increase. Therefore, this can prove that the premixed gas is already ignited, and combustion can be stabilized in the micro-combustion chamber with a gap of 2 mm.

In our experiments, six hydrogen flow rates were tested: 3.805×10^{-4}, 5.228×10^{-4}, 6.353×10^{-4}, 7.512×10^{-4}, 1.019×10^{-3}, 1.293×10^{-3} g s^{-1}, and the corresponding total thermal powers (Q_t) obtained from the fully combusted fuel were 46.0, 63.2, 76.8, 90.8, 123.2, 156.3 W, respectively. At each hydrogen flow rate, the excess air ratio α can be changed by gradually regulating the air flow rate. When the excess air ratio α is less than a certain value, the flame is suddenly quenched. The excess air ratio α under this status is named the minimum combustion limit. Correspondingly, when the air flow rate is gradually increased to a certain value, the flame is suddenly blown

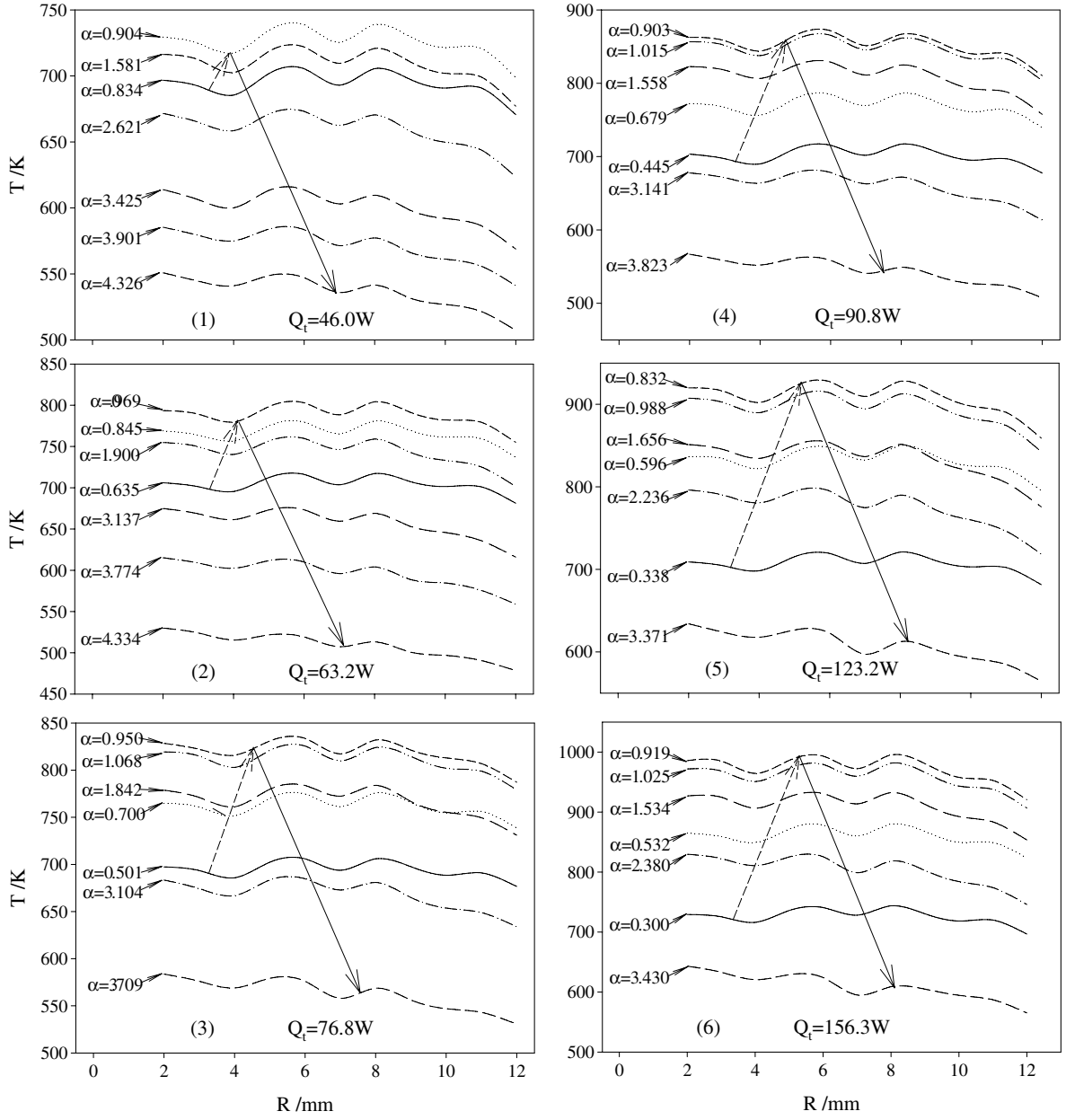

Fig. 4. Wall temperature fields of micro-combustor versus radius at different excess air ratio and thermal powers.

out. The excess air ratio α under this status is named the maximum combustion limit. Fig. 3 shows the minimum combustion limits and the maximum combustion limits at different thermal powers. From this figure, it is easily observed that the operating range of the combustor is very wide, and the maximum combustion limit is almost up to 4.5. At a higher excess air ratio, although the fuel mixture gas becomes lean, micro-combustion can still be maintained steady in the micro-combustor with a gap of 2 mm.

4.2. Wall temperature fields of the micro-combustor

The temperature fields of the micro-combustor wall were measured with some K type thermocouples at different thermal powers and different excess air ratios. Fig. 4 illustrates the distribution of the temperature fields with excess air ratio at different thermal powers. The outer wall temperature of the micro-combustion chamber rises with the increase of thermal power and is near 1142 K at the thermal power (Q_t) of 156.3 W.

It is obviously seen from Fig. 4(4) that at each hydrogen flow rate, the wall temperature of the micro-combustion chamber gradually increases with increasing excess air ratio from 0.445 to 0.903 and then begins to decrease with continually increasing excess air ratio from 0.903 to 3.823. The same phenomenon can also be observed in other conditions. Therefore, the wall temperature reaches the maximum value at the excess air ratio of about 0.9 instead of 1 (stoichiometric ratio). It is very interesting that the same results can be obtained in the silicon based micro-combustor [11]. The wall temperatures and exhaust gas of the silicon based micro-combustor reach the maximum value at the fuel/air ratio of about 1.2 (at the excess air ratio of about 0.84 correspondingly). Therefore, it is experimentally concluded that the temperature of the micro-combustor wall and exhaust gas reach the maximum value at the excess air ratio of about 0.9 instead of 1. It is well known that for conventional combustors, fuel and air can be burned fully at the stoichiometric ratio and all thermal energy is given off to heat the exhaust gas, and therefore, the temperature of the exhaust gas and combustor wall must reach the maximum value at the excess air ratio of 1 (stoichiometric ratio). However, for micro-scale combustion, the law is no longer satisfactory. The detailed mechanism that can explain this surprising phenomenon should be investigated further.

In addition, it is also known that a highest temperature point of the micro-combustion chamber wall is located not at 10 mm but about 8.5 mm away from the center. Numerical simulations were performed on the 3D geometries of the micro-combustor using FLUENT V6.18 software [12] of FLUENT Company with a nine species, 19 step hydrogen–air reaction mechanism [13] and species transport model. Fig. 5 shows the CFD generated velocity vector fields of a radial section of the micro-combustor at the excess air ratio of 1.558 and thermal power of 90.8 W. From Fig. 5, it is clearly seen that after being jetted from the 300 μm orifices distributed at 10 mm away from the center into the combustion chamber, the flame begins to change its direction and flows toward the center. The flame impacts the wall of the combustion chamber at about 9 mm away from the center. Moreover, the flow field of the micro-combustor is also disturbed by the heating wire located at 18 mm circumference. Therefore, the relatively high wall temperature zone is located not at 10 mm but at about 8.5 mm away from the center. In addition, it is also seen from Fig. 5 that the flame jetted from the 300 μm orifices at very high velocity, forms many high temperature recirculation zones around the orifice. Because the high temperature flame in the recirculation zones can successively ignite the lean fuel mixture gas from the micro-orifices, the operating range of the micro-combustor is greatly expanded with the help of the high temperature recirculation zones.

4.3. Heat loss of the micro-combustor

When the characteristic size of a combustor is down to a millimeter or micron scale, the surface area to volume ratio will increase greatly and be two orders of magnitude larger than that of a conventional combustor [2], and correspondingly, the heat loss via natural convection heat transfer and radiant heat transfer will increase greatly. As a result, the efficiencies of the micro-combustor and micro-gas turbine engine will be decreased due to the higher heat loss. Therefore, heat loss is an important factor for the micro-combustor, and more attention should be paid to reduce it.

The heat loss of the combustor to the environment consists of natural convection heat loss (Q_{nc}) and radiant heat loss (Q_r), which were calculated in terms of the wall temperature of the combustor and the ambient temperature. The total heat loss is the summation of the natural

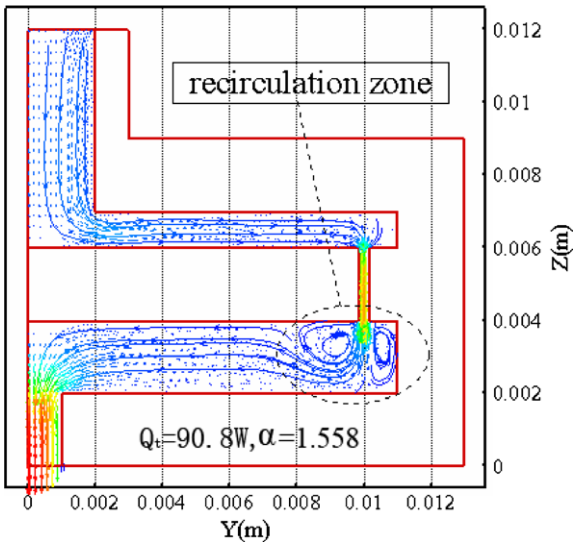

Fig. 5. Velocity fields of micro-combustor at excess air ratio of 1.558 and thermal power of 90.8 W.

convection heat loss (Q_{nc}) and radiant heat loss (Q_r). The rate of natural convection heat loss η_{nc}, the rate of radiant heat loss η_r and the rate of total heat loss η_t are, respectively, defined as percentages of the natural convection heat loss Q_{nc}, radiant heat loss Q_r and total heat loss ($Q_{nc} + Q_r$) in the total thermal power (Q_t) and can be written as

$$\left.\begin{aligned} \eta_{nc} &= \frac{Q_{nc}}{Q_t} \\ \eta_r &= \frac{Q_r}{Q_t} \\ \eta_t &= \frac{Q_{nc}+Q_r}{Q_t} \end{aligned}\right\} \tag{12}$$

Fig. 6 illustrates the distribution of the rate of natural convection heat loss η_{nc}, the rate of radiant heat loss η_r and the rate of total heat loss η_t with excess air ratio at different thermal powers.

It is known from Fig. 6 that the heat loss to the environment covers a considerable fraction of the total heat power (Q_t), even the maximum total heat loss is near 70% of the total heat power (Q_t). Only a fraction of the useful thermal power can be used to heat the exhaust gas and finally be converted to electrical energy. Therefore, the conversion efficiency from thermal energy to electrical energy for a micro-gas turbine generator will be largely reduced due to the considerable heat loss to the environment.

It is also seen from Fig. 6 that when the excess air ratio is up to about 0.9, the heat loss will reach its maximum

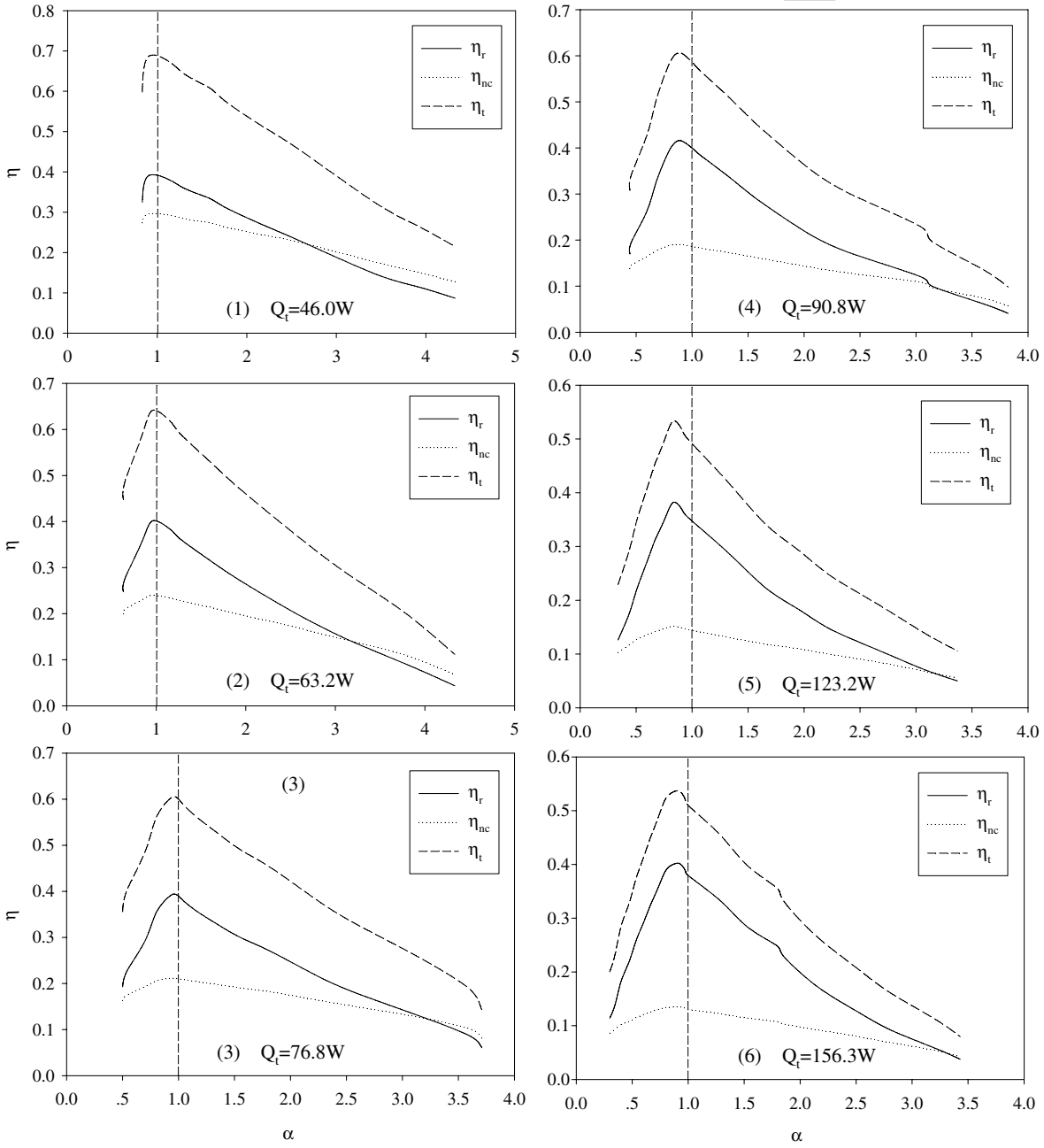

Fig. 6. Heat loss versus excess air ratio at different thermal powers.

value. Because the wall temperature of the micro-combustor reaches the maximum value at an excess air ratio of about 0.9, the natural convection heat loss and radiant heat loss to the environment are bound to increase to the peak value correspondingly. With the increase of the excess air ratio, the heat loss begins to decrease due to the reduction of the wall temperature of the combustor. In addition, we can also know from Fig. 6 that, compared with the natural convection heat loss, the radiant heat loss covers a greater fraction of the total heat loss. Specially, under the condition of higher thermal power, the radiation heat loss covers a larger fraction of the total heat loss, even exceeding 70%. Therefore, in order to enhance the thermal efficiency of the micro-combustor and conversion efficiency of the micro-gas turbine generator, the heat loss, especially the radiant heat loss to the environment must be reduced effectively.

In order to reduce the heat loss to the environment, some feasible methods are proposed: Firstly, an improved micro-combustor design with heat recirculating jacket should be adopted. On the one hand, the premixed gas through the heat recirculating jacket can insulate the micro-combustor from the environment and hinder a portion of the radiant heat loss to the environment. On the other hand, a portion of the heat loss can pre-heat the premixed gas in the heat recirculating jacket and finally be brought back to the micro-combustor. Without question, the heat recirculating jacket will help to enhance the efficiency of the micro-combustor. Secondly, reducing the emissivity of the wall surface of the micro-combustor can effectively decrease the radiant heat loss to the environment. The emissivity of the wall surface can be reduced by coating a layer of special material with lower emissivity on the wall surface of the micro-combustor. Thirdly, some special materials with lower thermal conductivity, such as ceramic, should be used to fabricate the combustor. Because employing some special material with lower thermal conductivity will increase the thermal resistance of the combustor wall, the heat loss by thermal conduction will be reduced. Finally, at higher thermal powers, micro-combustion should be operated at higher excess air ratios. Because at higher excess air ratio, the temperature of the micro-combustor wall is lower and, correspondingly, the heat loss to the environment will decrease.

4.4. Temperature of exhaust gas

The temperature of the exhaust gas of the micro-combustor is measured with a K type thermocouple, which is located at the center of the exit hole with a diameter of 2 mm, at a distance of 1 mm from the outer wall of the micro-combustion chamber. Fig. 7 illustrates the variety of temperatures of the exhaust gas of the micro-combustor with excess air ratio at different thermal powers. It can be seen from the figure that the temperature of the exhaust gas of the micro-combustor increases gradually with increasing excess air ratio from the minimum value. However, when the excess air ratio exceeds 0.9, it begins to decrease gradually. Just as the variety of temperatures of the micro-combustor wall, the temperatures of the exhaust gas also reach their maximum value at the excess air ratio of 0.9.

The compression ratio and temperature of the exhaust gas are two primary factors for enhancing the efficiency of the gas turbine. The higher is the temperature of the exhaust gas of the combustor, the higher is the efficiency of the gas turbine. Therefore, in order to obtain the higher temperature of the exhaust gas, on the one hand, micro-combustion should be operated at the excess air ratio of about 0.9. On the other hand, the micro-combustor should be operated at as high as possible thermal powers. It is seen from Fig. 7 that the temperature of the exhaust gas of the micro-combustor will also increase further with continuing increase of thermal power. The highest temperature of the exhaust gas reaches 1142 K when the thermal power is increased to 156.3 W, and the excess air ratio is about 0.9. However, if the thermal power is increased further, the temperature of the exhaust gas of the micro-combustor will also increase further, even exceeding the serviceable range of the material used to fabricate the micro-turbine blades and finally leading to failure of the material. Hence, at higher thermal powers, micro-combustion can only be operated at higher excess air ratios, so that the temperature of the exhaust gas of the micro-combustor can be lower than the serviceable range of the material of the micro-turbine blade. Because the operating range of the micro-combustor is very wide and even the maximum excess air ratio exceeds 4.5, appropriately increasing the excess air ratio at the higher thermal powers can easily control the temperature of the exhaust gas of the micro-combustor. Ideally, micro-combustion should be operated at the excess air ratio where the temperature of the exhaust gas of the micro-combustor is controlled to be a bit less than the serviceable range of the material of the micro-turbine blade.

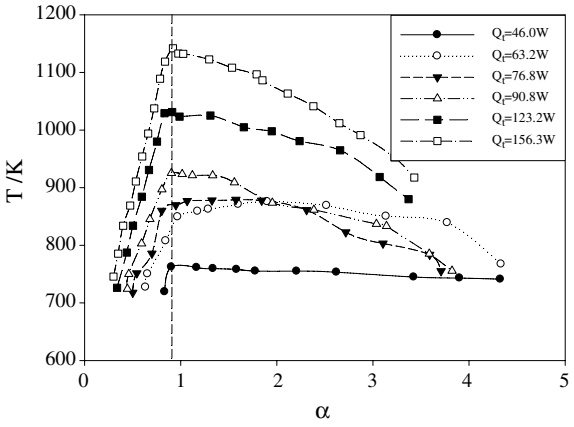

Fig. 7. Temperature of exhaust gas versus excess air ratio at different thermal powers.

5. Conclusions

Premixed combustion experiments of hydrogen gas and air were performed in a stainless steel based micro-annular combustor, and micro-combustion can be stabilized in the micro-combustor with a gap of 2 mm. The operating range of the micro-combustor is measured at different thermal powers, and it is experimentally proved that micro-combustion can be stabilized for a wide operating range.

In the experiment, we measured the wall temperature of the micro-combustion chamber and the exhaust gas temperature of the micro-combustion and found that the wall temperature of the micro-combustor and the temperature of the exhaust gas of the micro-combustor reach their maximum values at the excess air ratio of 0.9 instead of 1 (stoichiometric ratio). The heat loss from the wall surface of the micro-combustor to the environment was calculated and analyzed at different thermal powers, and it was proved to cover a great fraction (even exceeding 70%) of the whole thermal power. Moreover, even the radiant heat loss can exceed 70% of the whole heat loss. Some methods were proposed to reduce the heat loss of the micro-combustor and, consequently, should be adopted in developing an improved micro-combustor.

In addition, the higher is the thermal power, the higher is the temperature of the exhaust gas of the micro-combustor. If the thermal power is increased and exceeds a certain value, the micro-turbine blades will be damaged due to an excessively high temperature of the exhaust gas. Therefore, at higher thermal powers, micro-combustion should be operated at an excess air ratio where the temperature of the exhaust gas of the micro-combustor is controlled to be a bit less than the serviceable range of the material of the micro-turbine blade.

References

[1] Epstein AH, Senturia SD, Anathasuresh G, et al. Power MEMS and microengines. In: Proceeding of international conference on transducer' 97, Chicago, vol. 2; 1997. p. 753–6.
[2] Spadaccini CM, Mehra A, Lee J, et al. High power density silicon combustion system for micro gas turbine engines. J Eng Gas Turbines Power 2003;125:709–19.
[3] Mehra A, Zhang X, Ayon AA, et al. A six-wafer combustion system for a silicon micro gas turbine engine. J Microelectromech Syst 2000;9(4):517–27.
[4] Yang WM, Chou SK, Shu C, et al. Microscale combustion research for application to micro-thermophotovoltaic systems. Energy Convers Manage 2003;44:2625–34.
[5] Yang WM, Chou SK, Shu C, et al. Combustion in micro-cylindrical combustors with and without a backward facing step. Appl Thermal Eng 2002;22:1777–87.
[6] Shan XC, Wang ZF, Jin YF, et al. Studies on a micro combustor for gas turbine engines. J Micromech Microeng 2005;15:S215–21.
[7] Wu M, Hua JS, Kumar K. An improved micro-combustor design for micro gas turbine engine and numerical analysis. J Micromech Microeng 2005;15:1817–23.
[8] Peirs J, Reynaerts D, Verplaetsen F. Development of an axial microturbine for a portable gas turbine generator. J Micromech Microeng 2003;13:S190–5.
[9] Fu K, Knobloch AJ, et al. Microscale combustion research for applications to MEMS rotary IC engine, In: Proceedings of NHTC, 2001 national heat transfer conference, Anaheim, CA. June 10–12, 2001. p. 1–6.
[10] Yang SM, Tao WQ. Heat transfer. 3rd ed. Beijing: Higher Education Press of China; 1998. 178–188, 243–245.
[11] Mehra A, Ayon AA, Waitz IA, et al. Micro fabrication of high temperature silicon devices using wafer bonding and deep reactive ion etching. IEEE J Microelectromech Syst 1999;8(2):152–60.
[12] Fluent Incorporated. Fluent 6.1 user's guide. vol. 2, February 2003. p. 13.1–.35.
[13] Markatou P, Pfefferle LD, Smooke MD. The influence of surface chemistry on the development of minor species profiles in the premixed boundary layer combustion of an H_2/air mixture. Combus Sci Technol 1991;79:247–68.